THE INFLUENCE OF ARCTIC SEA ICE EXTENT ON POLAR CLOUD FRACTION AND VERTICAL STRUCTURE AND IMPLICATIONS FOR REGIONAL CLIMATE

Stephen P. Palm[1], Sara T. Strey[2], James Spinhirne[3] and Thorsten Markus[4]

[1]Science Systems and Applications, Inc.

[2]University of Illinois

[3]University of Arizona

[4]Goddard Space Flight Center

Abstract

Recent satellite lidar measurements of cloud properties spanning a period of five years are used to examine a possible connection between Arctic sea ice amount and polar cloud fraction and vertical distribution. We find an anti-correlation between sea ice extent and cloud fraction with maximum cloudiness occurring over areas with little or no sea ice. We also find that over ice free regions, there is greater low cloud frequency and average optical depth. Most of the optical depth increase is due to the presence of geometrically thicker clouds over water. In addition, our analysis indicates that over the last 5 years, October and March average polar cloud fraction has increased by about 7 and 10 percent, respectively, as year average sea ice extent has decreased by 5 to 7 percent. The observed cloud changes are likely due to a number of effects including, but not limited to, the observed decrease in sea ice extent and thickness. Increasing cloud amount and changes in vertical distribution and optical properties have the potential to affect the radiative balance of the Arctic region by decreasing both the upwelling terrestrial longwave radiation and the downward shortwave solar radiation. Since longwave radiation dominates in the long polar winter, the overall effect of increasing low cloud cover is likely a warming of the Arctic and thus a positive climate feedback, possibly accelerating the melting of Arctic sea ice.

1 Introduction

In recent years, much attention has been given to the Arctic because of its sensitivity to climate change. Evidence of change has been seen at an accelerating rate over the last decade or more. Surface temperatures, though scarce in the Arctic, show a 1-2 degree C increase over the last 20 years [Rigor et al., 2000]. During this period, Arctic sea ice extent has decreased by an average of 15 to 20 percent [Serreze et al., 2007]. Dramatic reduction in the thickness of the remaining sea ice has also been measured over the last decade [Kwok, 2009]. The decrease in sea ice extent and subsequent increase in open water will have two immediate effects: 1) an increase in the surface fluxes of heat and moisture from the ocean to the atmosphere and 2) a marked decrease the surface albedo. The first effect will tend to cool the ocean and moisten and warm the atmosphere, possibly leading to changes in cloud properties such as coverage, vertical structure, phase, and optical depth. The second effect will allow more solar radiation to be absorbed at the surface, thereby heating the ocean. These combined effects could have implications for regional climate and larger scale weather patterns as well. Changes in cloud properties could have profound effects on radiative balance. For instance, Shupe and Intrieri, [2004] found that cloud longwave and shortwave forcing were related to cloud fraction based on

year-long measurements over pack ice during SHEBA (Surface Heat Budget of the Arctic). Further, they found that an increase in cloud fraction will impart greater surface warming relative to current conditions for most of the year, except for a few weeks in midsummer when the shortwave cooling dominates longwave warming.

In addition to regional changes in clouds and radiative forcing, a number of studies, both theoretical [Deser et al., 2007; Alexander et al., 2004]) and observational [Francis et. al., 2009], have found connections between Arctic sea ice extent and general circulation and precipitation patterns. Francis et al. [2009] show that there are measurable effects of decreased summertime Arctic sea ice extent on surface pressure and precipitation in the following autumn and winter including locations far from the Arctic. Presumably, these effects may in some way be related to the increased fluxes of heat and moisture from the surface to the atmosphere [Bhatt et. al., 2008]. However, the exact cause of these effects is not fully known. Obviously, the changes in sea ice extent and thickness now ongoing in the Arctic warrant a close examination of its effect on the atmosphere and on recent polar cloud trends.

There have been a number of studies examining the trend of Arctic cloudiness over the last few decades, but often, prior work on Arctic cloud changes has led to conflicting conclusions. Schweiger et al., [2008] used passive observations from TOVS (TIROS Operational Vertical Sounder) and the 40 year ECMWF Re-Analysis (ERA-40). They found that sea ice retreat was linked to a decrease in low-level cloud amount and a simultaneous increase in mid level clouds near the ice margins. Wang and Key [2003] and Schweiger [2004] used AVHRR derived cloud datasets to conclude that the springtime cloudiness is increasing with time while conversely, Comiso [2003] used a separate AVHRR data set and found springtime cloudiness is decreasing. Kato et al., [2006] found an increase in Arctic cloudiness over the period March 2000 to February, 2004 using Moderate Resolution Imaging Spectroradiometer (MODIS) data with a trend of 4.7% per decade. While significant sea ice reduction was seen during this period, the top of the atmosphere short wave irradiance changed very little, indicating increased cloudiness was offsetting the albedo lowering effect of reduced sea ice extent. Surface observations of clouds have generally shown an increase of polar cloud amount regardless of season (Eastman and Warren [2010]). The ambiguity in the satellite results and the disagreement with surface observations may be attributable to the passive cloud detection techniques employed. It is very difficult to obtain accurate cloud detection over ice from passive instruments. Active remote sensors such as lidars are not affected by problems that can often hamper passive cloud retrievals such as the underlying surface albedo, lack of sunlight and atmospheric temperature inversions. Evan et al. [2008] utilize CALIPSO and CloudSat data to show that the anomalously low cloud amount in summer, 2007 was followed by greater than average cloud fraction in early fall. They further note that during 2007, the clouds had a lower base height and that midlevel cloud amount increased. Intrieri et al. [2002] give a comprehensive report on ship-based lidar and radar measurements of clouds during SHEBA but the data do not span a long enough time to discern trends. Otherwise, an extensive analysis of how Arctic cloud properties have been changing in recent years using data from active remote sensing has been limited. A notable exception is Kay and Gettelmen [2009] who used CloudSat and CALIPSO data in conjunction with other passive sensors to examine cloud responses to and influences on seasonal Arctic sea ice loss for the period 2006 to 2008.

This study utilizes satellite lidar data from the Ice, Cloud and land Elevation Satellite (ICESat) and the Cloud-Aerosol Lidar and Infrared Pathfinder Satellite Observations (CALIPSO) to ascertain changes in Arctic clouds since 2003. Emphasis is placed on cloud fraction, vertical structure and optical thickness over ice free versus ice covered areas. The overall radiative effect of clouds will depend on their fractional coverage, height, geometric and optical thickness, vertical structure and water phase. Additionally, we will use these findings to infer what effect the reduced ice cover in the Arctic has on the radiative balance and Polar climate. Section 2 discusses the data sets utilized in this study and Section 3 looks at the Arctic cloud fraction as derived from ICESat and CALIPSO and its relationship to Arctic sea ice extent. Section 4 will address the vertical distribution of Arctic clouds and cloud optical depth to determine if there are any changes in these properties over ice covered regions versus open water. Summary and conclusions are then given in Section 5.

2. Satellite Data Sets

ICESat was launched in 2003 to study the mass balance of the earth's major ice sheets. Onboard ICESat is the Geoscience Laser Altimeter System (GLAS) comprised of a high precision surface altimeter channel [Schutz et al., 2005] and two atmospheric lidar channels (1064 and 532 nm) used to detect clouds and aerosols [Spinhirne et al., 2005]. Although designed to obtain measurements continuously for a period of 3 years, laser problems encountered shortly after launch required a modified observation approach consisting of month-long measurement periods executed three times per year. The ICESat cloud height data set utilized here is known as GLA09 and is publicly available at the National Snow and Ice Data Center (NSIDC). We used the version 28 cloud heights at 1 and 4 second resolution (7 and 28 km, respectively) derived from the 1064 nm channel which was more stable in laser energy than the 532 nm channel. Though ICESat continued to operate until the first part of 2009, we do not use the cloud data past October of 2007 (ICESat observation period known as L3I), because of low laser energy.

CALIPSO is a dual wavelength atmospheric lidar similar to GLAS and has been in continuous operation since June of 2006 [Winker et al., 2007]. The cloud data set used in this study is from version 2 of the level 2B data obtained from the NASA Langley Atmospheric Science Data Center. The cloud heights were derived from the 532 nm channel of CALIPSO. We used only the 5 km and 20 km cloud resolutions in compiling the CALIPSO cloud statistics. There is a period from June, 2006 to November of 2008 that provides limited (4) opportunities to compare the CALIPSO cloud retrievals to those of GLAS. These show very good agreement with cloud percentage differences (ICESat – CALIPSO) of 1.0, 0.2, -2.4 and 1.5. This will be further explored in Section 3.

Though the lidar active remote sensing technique has its advantages (namely vertical accuracy and insensitivity to lack of sunlight or thermal contrast), the main disadvantage is its limited spatial coverage. Both CALIPSO and ICESat obtain data only directly below the orbit track at nadir. Fortunately, in the polar regions, the spatial sampling density is greater than at lower latitudes. Since we utilize measurements from both satellites in constructing a time series of cloud fraction, we should also mention that their orbital parameters differ considerably which affects both the spatial sampling density and the local sampling time. CALIPSO is part of the A-

Train satellite constellation and is in a sun-synchronous orbit with an inclination of 98 degrees (enabling measurements to be obtained to 82 N). ICESat's orbit has an inclination of 94 degrees (enabling measurements to be obtained to 86 N) and is not sun-synchronous. This means that the CALIPSO measurements are obtained at roughly the same local time over a given region, throughout the lifetime of the satellite, while the local time of ICESat's measurements will vary from one observation period to the next. While this difference in local sampling time would be a concern over land, we do not think it has much of an effect on the cloud statistics over the Arctic Ocean utilized here. The difference in orbit inclinations will have an effect on the sampling density in the Arctic region, producing more CALIPSO observations than ICESat observations (since we are eliminating the ICESat measurements above 82 N). These differences can have an effect on the retrieved cloud distribution and thus make it difficult to combine the cloud statistics of the two into one long time series as is done here. In an effort to better quantify such differences, we present an analysis of overlapping ICESat and CALIPSO cloud fraction retrievals from the Arctic and various regions in the Atlantic and Pacific Ocean in Section 3.

Sea ice coverage is derived from the Advanced Microwave Scanning Radiometer (AMSR-E) on the EOS Aqua satellite launched in May, 2002 [Comiso et al., 2003]. The instrument provides daily coverage of the entire Arctic Ocean at a spatial resolution of 12.5 km. In this analysis, we use the AMSR-E monthly average sea ice amount, which is given in terms of percent coverage of the study area.

3. Arctic Cloud Fraction

This study seeks to determine trends and relationships between sea ice coverage and Arctic cloud properties. As such, we limit our analysis of polar clouds to areas between 60 N and 82 N and to areas over ocean and sea ice (heretofore the study area). The land/ocean mask available in both the GLAS and CALIPSO data products is used to segregate the cloud data so that only cloud data over water or ice is considered in the analysis. An example of cloud fraction retrieval over the study area is shown in Figure 1. Displayed are the cloud fraction obtained from ICESat and CALIPSO for the period October 2 to November 5, 2007 and the sea ice fraction for the month of October, 2007 based on AMSR-E data. The cloud fraction maps are obtained by constructing a 1 by 1 degree grid over the study area and counting all detected clouds within each grid box for the period and dividing this count by the number of satellite observations for that grid box. Generally, each grid box contains about 30 to 40 observations (per 33 day observation period) for CALIPSO and somewhat less for ICESat. This is dependent on latitude, however, with higher spatial sampling in the highest latitudes. Because grid box size is larger than the intrinsic horizontal resolution of the cloud measurements (about 20 km), multiple observations from a single orbit pass are often accumulated in a given grid box. Thus, Figure 1 represents more of a composite of cloud fraction, rather than a true average since there are many grid boxes with less than 1 observation per day. From Figure 1, two things are evident: 1) ICESat and CALIPSO are measuring nearly the same spatial cloud distribution and amount and 2) there is an apparent anti-correlation between cloud fraction and sea ice amount (calculated to be -0.31). Though cloudiness is very high over the entire Arctic, it is generally 10 to 15 percent greater over areas with little or no sea ice (less than 20 percent ice coverage) than it is over regions with high sea ice concentration (greater than 80 percent). In areas of open water, cloudiness is often near 100 percent. This observation is consistent with increased surface fluxes

in areas of open water and the work of Strey et. al. [2010] shown in Figure 4 and discussed in section 4. While there are other factors that regulate cloud formation and amount, the surface boundary condition has a large influence. Also, the compositing period of one month used here helps to remove the high frequency variability of cloudiness due to the synoptic scale weather systems leaving mainly the influence of the surface boundary condition. Occasionally, however, large scale weather patterns may persist for periods longer than a month as they did over the Arctic in the summer of 2007 when anomalously low cloud fraction was observed over much of the Arctic by CALIPSO and other satellites during June and July. Kay et al., [2008] suggest that this low cloud amount allowed an increased amount of solar energy to warm the surface and helped to contribute to the record sea ice melt during the late summer of 2007. While Perovich et al., [2008] conclude that increased solar radiation absorbed in the upper ocean (due to lower albedo associated with more open water and a modest 6% increase in shortwave radiation at the surface) during the summer of 2007 contributed to accelerating ice retreat, others such as Schweiger et al.,[2008] and Kauker et al., [2008] have found through model experiments that reduced cloud cover and the resulting increase of absorbed solar radiation in the summer of 2007 played only a minor role in the 2007 record ice extent minimum.

Utilizing the entire data record of ICESat and CALIPSO, a 63 month-long history (though not continuous) of cloud fraction over the Arctic can be constructed. Figure 2 shows the average cloud fraction obtained from all ICESat observation periods since October, 2003 and ending in October, 2007 (pink crosses). Most of the ICESat observation periods were roughly 33 days long and tended to occur during the months of February-March, May-June and October-November. Also plotted in Figure 2 is the monthly average cloud fraction for the study area derived from CALIPSO measurements (solid dark black line) and the AMSR-E derived sea ice coverage in percent of study area (solid red line). Readily visible is the yearly cycle in sea ice amount and cloud fraction. Both of these cycles are well known, but the latter is more difficult to explain, and arises from a number of different reasons. Beesley et al., [1999] point to three major causes of the cloud fraction cycle in the Arctic: 1) moisture flux convergence, 2) surface evaporation (which is controlled mainly by the presence/absence of sea ice), and 3) temperature dependent ice-phase processes. Their model results suggest that the 3rd factor is most important in regulating cloud amount in the Arctic. This work indicates that even though there is a strong anti-correlation between cloud fraction and sea ice amount in Figure 2, there is not necessarily a cause and effect relationship between the two. While it plays a role, the work of Beesley et al. implies that it is not the increased surface moisture flux from open water that is the major cause of the increase in summertime clouds in the Arctic.

As mentioned previously, in Figure 2 there are four ICESat observation periods for which exist corresponding CALIPSO measurements and that the agreement in cloud amount between the instruments is generally good (mean difference and standard deviation of 1.2 and 0.9 percent, respectively). Also shown in Figure 2 is the linear least square fit to all of the October cloud fraction data points (both ICESat and CALIPSO, upper thin, straight black line). The slope of this line indicates that the October cloud fraction has increased by about 6-7 percent over the observation period, or about 13 percent per decade. Following the method used in Santer et al. [2000], this trend was determined to be significant at the 95% level. However, when combining cloud measurements from two different satellites care must be taken to characterize any bias between them. We attempt to compute the bias by comparing ICESat and CALIPSO cloud fractions for the Arctic (for all 4 overlapping observation periods) and 4 additional regions

around the globe for two of the ICESat observation periods that overlapped with CALIPSO (October – November, 2006 and February – March, 2007). For all of these periods for the Arctic and each of the 4 sub-regions, the cloud fraction mean for both satellites was calculated. The additional sub-regions chosen for the analysis consisted of 40 degree by 40 degree boxes in the North and South Atlantic and Pacific Ocean so as to minimize diurnal differences in cloud amount that might occur more strongly over land (since CALIPSO and ICEsat have different equator crossing times). The results are shown in Table 1. On average, ICESat retrievals yield a cloud fraction slightly larger than CALIPSO (1.5%). The RMS of the difference between the two cloud fraction measurements is 2.8%. These figures indicate that ICESat's cloud fraction retrievals are not biased low with respect to CALIPSO and the increase in cloud fraction with time shown in Figure 2 cannot be attributed to a detection sensitivity difference between the two instruments. The difference of the cloud fraction means (1.5%) shown in Table 1 can be used as a measure of uncertainty in the trend of cloudiness that is inferred from the combination of these two cloud data sets. The linear least square fit to the October AMSR-E sea ice extent data points is also shown in Figure 2 (lower, straight orange line) and indicates a roughly 6 to 7 percent decrease in sea ice over the 5 year period. While this rate of decrease is somewhat larger than other published figures (10 percent per decade [Stroeve et al., 2007]) it may not be unreasonable considering the accelerating rate of decline in the last 2 to 3 years of this 5 year period (2003 to 2008).

The dashed black line in Figure 2 denotes the CALIPSO cloud fraction for the sub-region bounded by 90° to 270° longitude and north of 70° latitude (this area includes the Laptev, East Siberian, Chukchi and Beaufort Seas). There are two things to note about the cloudiness in this region. 1) The wintertime minimum in cloudiness is considerably lower than for the whole Arctic region, while the summer and fall maximum in cloudiness is about the same. 2) June and July of 2007 experienced lower cloud fraction in the sub-region than the Arctic region as a whole, though the latter region cloud amount was considerably less than the values for June and July of either 2006 or 2008. It is in this sub-region that a large amount of melting occurred during the late summer of 2007. Kay et al. [2008] attribute this melting at least in part to the anomalously low cloud amount over the region in June and July caused mainly by a stationary high pressure area with widespread subsidence. This allowed a higher than normal amount of solar radiation to reach the surface. Initially, most of the sunlight will be reflected from the ice, but as the ice melts and water ponds form, the albedo decreases allowing more of the incoming solar radiation to be absorbed. The more the ice melts, the more shortwave radiation is absorbed and the melting accelerates. If, however, clouds form in response to the increased open water, this process would be affected because the clouds will reflect much of the shortwave radiation. Kato et. al. [2006] report observing an increase in reflected shortwave radiation from MODIS data associated with increased Arctic cloud cover from 2000 to 2004. In June and July, 2007 cloud amount was low, but note that the cloud amount in the sub-region increased dramatically in August and September, 2007 from about 70% in July to 93% in September, possibly due (at least in part) to the increase in open water during August and September. Of course, a full analysis of the cause must include an examination of the synoptic scale meteorological conditions present during this period. It should also be noted that the 2007 and 2008 wintertime (Dec – Mar) cloud fraction in this sub region closely follows the observations obtained during the SHEBA experiment in 1998 reported in Intrieri et al. [2002]. Their data show an average yearly cloud fraction of about 80% with a minimum of about 65% during February to March and a maximum between 90 to 95% in the summer months. In comparison, the December to March

CALIPSO observations for the sub region show an average cloudiness of about 68% for 2007 and 63% for 2008 and summertime cloudiness averages about 90%.

Another interesting thing to note from Figure 2 is the marked increase in March cloudiness for the study region as a whole during the period shown. ICESat data from 2006 and earlier show an average March cloudiness of 60 to 65%, while after this time the ICESat and CALIPSO measurements indicate cloudiness has increased to about 73%. A linear least square fit through all the March data points (ICESat and CALISPO) yields an increase in cloudiness of 10% for the period shown (March 2004 through March 2008), which is significant at the 99% confidence level. Liu et al., [2007] and Wang et al., [2005] found a decrease in winter (Dec, Jan, Feb) Arctic cloudiness based on an analysis of AVHRR data for 1982 to 1999, but an increase in spring (Mar, Apr, May) and summer. Thus, it is not clear how the March trend observed here compares with their results. It should be noted, however, that the retrieval of clouds from passive observations is affected by the underlying surface albedo [Liu et al., 2010, Mahesh et al., 2004]. Computation of the trend in Arctic cloud fraction by passive measurements is thus affected by the trend in Arctic sea ice. This effect is most pronounced in summer and early fall when sea ice extent has seen the greatest decrease.

4. Cloud Vertical Distribution and Optical Depth

In addition to cloud amount, the vertical distribution and properties of clouds are also very important in determining the affect they have on radiative forcing. If low cloud base relative to high cloud base increases, the overall effect can be one of increased radiation heating at the surface even for the same cloud fraction. Lidar provides a valuable technique for retrieving cloud vertical structure, phase (if depolarization channel is present as for CALIPSO), and optical depth (of thin clouds). The one drawback of spaceborne lidar observations to determine cloud vertical structure is that low clouds can potentially be shadowed by the presence of higher, attenuating clouds, resulting in an under representation of low clouds. For both ICEsat and CALIPSO, full attenuation of the laser beam occurs at an optical depth of about 3 to 4. This means that the true bottom of clouds with optical depth greater than this cannot be obtained. In the polar regions, this generally occurs only for low stratus clouds which are often not geometrically thick. If a cloud is optically thick (> 3) but not thick geometrically, then the bottom obtained from the lidar backscatter will be higher than the actual cloud bottom, but not by a large amount. We therefore, do not expect this effect to change the average cloud vertical distribution appreciably. Shadowing of low clouds due to overlying optically thick clouds will render the low clouds invisible and thus affect the vertical frequency distribution, but for the Arctic we believe this to be a relatively small percentage of the cloud retrievals. Despite these limitations, lidar measurements of cloud frequency as a function of height can be very informative. In Figure 3 we have created a histogram of the average lidar cloud height ((top+bottom)/2) (or frequency of occurrence) as a function of height of Arctic clouds as derived from the five October ICESat observations from 2003 through 2007. Also shown is the vertical distribution of average cloud optical depth for the same clouds and time period. The cloud retrievals have been segregated into those that occur over areas with ice concentration greater than 80% (dashed line) and those that occur over regions where the ice concentration is less than 20% (solid line). For the cloud frequency plot (Figure 3a), they have also been normalized by the number of clouds detected in each segregated population. Note that when shown in this way, the curves do not show the true number of clouds relative to each other, but rather how the clouds in

each population are distributed vertically. There are distinct differences in the cloud vertical frequency and optical depth of the two populations. The vertical distribution of clouds over water peaks somewhat higher in the atmosphere at a lower frequency of occurrence than for the clouds over ice. However, the frequency distribution of clouds over water below 2 km is broader, indicating more clouds between about 800 and 1800 m altitude. This is most likely due to a de-stabilization of the lower troposphere and deepening of the boundary layer caused by increased surface fluxes over the open water. This observation is somewhat different but consistent with the conclusion of Schweiger et al. [2008] who found a decrease in clouds below 800 hPa (roughly 2 km) and an increase in cloud amount between 800 and 450 hPa (roughly 2 to 6 km) as ice cover retreated. The conclusion from our analysis indicates that over open water the number of very low clouds (less than 500 m) decreased, while the number of clouds between 500 m and 2 km increased significantly. The difference between our analysis and the findings of Schweiger et al., [2008] could be due to the limitations of assigning height values to clouds via passive remote sensing. In addition, our results in Figure 3 indicates less clouds over water between 2 and 4 km, but that above 4 km there is a slightly higher frequency of clouds over water than over ice.

In addition to the changes in cloud vertical distribution, Figure 3b indicates that there is a 20 to 30 percent increase in the optical depth of the clouds over open water, but only above 1 km altitude. This is at first glance difficult to explain, but further analysis indicates that the increased optical depth is due mainly to the fact that clouds are geometrically thicker, on average, over water than over ice. The average backscatter (not shown) does not differ significantly between the two groups. This geometric thickness difference between the two populations decreases as clouds become lower and thus the optical depths converge below about 1 km.

The differences in the measured vertical cloud distribution over ice versus over water are most likely related to the surface boundary condition. Modeling studies have shown both an increase in boundary layer height and higher surface fluxes associated with sea ice retreat [Bhatt et al., 2008; Alexander et al., 2004]. Sea ice extent reached an all-time minimum in the summer of 2007. In an effort to better understand the impacts of such dramatic sea ice loss on the atmosphere, we employed the Weather Research and Forecast model (WRF) Advanced Research WRF (ARW) version 3.0.1 [Skamarock et al., 2008]. Two sets of ten simulations were run to determine the effects of reduced sea ice extent on the atmosphere including surface fluxes, boundary layer height and precipitation. The first set of model runs were made with 2007 atmosphere and sea ice boundary condition forcing and the second set with 2007 atmosphere boundary forcing but 1984 sea ice extent. Both sets of simulations were forced with NCEP reanalysis data and ran from September through December. Averaged over both sets of ensembles, the largest difference between the two cases occurred in October. At this time of year, the length of darkness is rapidly increasing and temperatures are falling leading to cold air interacting with open water. In these areas where cold air interacts with warm water we see an increase in upward latent heat flux and boundary layer height as seen in Figure 4a and b respectively. The decreased sea ice amount in this region in 2007 compared to that of 1984 causes the large surface heat flux and boundary layer height increases seen in the western Arctic Ocean. Note that the maximum boundary layer height difference in Figure 4b approaches 300 m. This is less than, but consistent with the shift in the peak of the vertical cloud distribution shown in Figure 3a (about 500 m). Changes in surface flux and boundary layer height can lead to other

atmospheric effects such as regional precipitation and temperature anomalies both in and far from the Arctic region [Strey, 2009; Strey et al., 2010; Bhatt et al., 2008].

5. Trend in Arctic Cloudiness and Consequences for Radiative Balance and Climate

Our observations indicate that areas of open water are associated with greater polar cloud fraction and that both March and October (and possibly yearly) average polar cloud fraction is increasing over the study period (2003 – 2008). In addition, there are significant differences in cloud properties (vertical distribution and cloud optical depth) depending on whether they occur over water or over sea ice. It follows that if Arctic sea ice cover continues to decline, polar cloud fraction will continue to rise. However, the rate at which it will increase is not totally clear. The overall increase in cloud fraction by a linear fit to the points in Figure 2 is about 6 to 7 percent per five years. A simple extrapolation of this rate would conclude that 100 percent cloudiness will be reached in 12 to 15 years (current year-round average Arctic cloudiness is about 82%). At that time, based on current sea ice loss rates, sea ice extent would be about 36 percent, down from the current value of 56%. (these values are yearly averages over the whole study area). The processes controlling cloud and sea ice interaction are not likely linear, however. Figure 5 shows the October cloud fraction points shown in Figure 2 plotted against their corresponding study area sea ice percentage. ICESat data from 2005 are not included since they span the period 10/21 to 11/24, and thus are more representative of November. Figure 5 plainly shows the anti-correlation of cloud amount with sea ice extent and that October cloudiness is increasing at a substantial rate from 2003 to 2008. If summer and early fall sea ice amount continues to decline into the future, we can expect October Arctic cloudiness to increase. So far, the cloud response looks linear, but it is unlikely that a linear trend will continue.

Vavrus et al., [2009] present an interesting study on future Arctic cloud changes in a warming earth using an ensemble of GCM model predictions. They find a strong dependence of cloud amount and cloud changes on sea ice cover. Maximum cloudiness occurs over open water in the summertime, though model cloud fraction values are lower (81%) than what is observed in this study (90%). The twenty GCMs used in the study show a large spread in simulated late 20th century annual polar cloud amount, ranging from 55 to 90% (ensemble mean of 76%). Under the assumed greenhouse forced warming scenario, the late 21st century annual polar cloud amount ranges from 65 to 92%, with an ensemble average of 79%. Maximum cloud increases occur during autumn, when an extensive area of 7–9% greater cloudiness is seen from North America to Siberia over the region coinciding with a large reduction (30%) in ice concentration during the late 21st century. The Arctic also becomes considerably cloudier during winter, and the increases are accentuated in the regions that experience the largest reductions in sea ice. These results are consistent with our observations, but the rate of which cloud polar fraction increases is considerably less than what our observations indicate has occurred over the period studied here (2003 – 2008).

As the Arctic cloudiness increases, we expect a decrease of down-welling shortwave radiation and an increase of down-welling longwave (LW) radiation. Since LW radiation dominates the surface energy balance through most of the year, we expect an increase of LW radiation at the surface to produce surface warming. For a short time in midsummer, the net down-welling radiation can be decreased because at mid-summer in the Arctic, the shortwave

component is larger than the longwave [Curry et al., 1996]. In the presence of increased cloud cover, less down-welling radiation could slow down the melting of sea ice in summer months. However, in winter an increased cloud amount could decrease the radiative cooling and slow down the freezing process, resulting in less thick ice at the end of winter. This would leave the ice more susceptible to melting the following summer.

Our results also suggest that the vertical distribution of clouds may change in response to sea ice melt with an increased fraction of the clouds (over open water) below 2 km, especially between 800 and 1800 m. However, the frequency of very low clouds (< 500 m) over open water decreased. This observation is consistent with the hypothesis of increased surface fluxes destabilizing the lower troposphere and creating a warmer, moister and deeper boundary layer over open water. The modeling study of Vavrus et al., [2009] also show increased low (925 hPa or roughly 1 km) polar cloud amount as climate warms and sea ice decreases. We find that cloud geometrical and optical thickness tend toward higher values over open water or low sea ice concentration areas. In addition to increased overall cloud fraction, the observed vertical cloud property distribution changes have the potential to alter the radiation balance of the Arctic. Increases in low cloud cover tend to produce cooling during summer months and a warming in the winter months. The change in surface temperature is not clear for late spring and early fall when the Arctic is sunlit, but the solar elevation is low. The total effect of cloud changes on radiative balance in the Arctic is complicated, and depends not only on cloud fraction, vertical distribution and optical depth but also on the water phase and particle size of the cloud droplets. While we did not address changes in the water phase of the clouds, CALIPSO depolarization data can be used to analyze water phase. Other instruments such as MODIS can be used to look for changes in particle size and changes in thick cloud optical depth. The rapid changes taking place in the Arctic call for further study that will require both continued observational and modeling studies.

6. Acknowledgments

The authors would like to recognize the NASA Langley Research Center Atmospheric Science Data Center for supplying the CALIPSO data used in this research. We also acknowledge valuable conversations with Dr. Alexander Marshak and Dr. Yuekui Yang of Goddard Space Flight Center.

7. References

Alexander, M. A., U. S. Bhatt, J. E. Walsh, M. Timlin, and J. S. Miller (2004), The atmospheric response to realistic Arctic sea ice anomalies in an AGCM during winter, *J. Climate*, *17*, 890-905.

Beesley, J. A., and R. E. Moritz, (1999), Toward an explanation of the annual cycle of cloudiness over the Arctic ocean. *J Climate, 12*, 395-415.

Bhatt, U. S., M.A. Alexander, C. Deser, J.E.Walsh, J.S. Miller, M. Timlin, J.D. Scott, and R. Tomas (2008), The Atmospheric Response to Realistic Reduced Summer Arctic Sea Ice Anomalies, in Arctic Sea Ice Decline: Observations, Projections, Mechanisms, and Implications, *Geophys. Monogr. Ser*., vol. 180, edited by E. T. DeWeaver, C. M. Bitz, and L.-B. Tremblay, pp. 91-110, AGU, Washington, D. C.

Comiso, J.C., (2003), Warming trends in the Arctic from clear sky satellite observations. *J. Climate, 16*, 3498-3510.

Comiso, J.C., D.J. Cavalieri and T. Markus (2003), Sea ice concentration, ice temperature, and snow depth using AMSR-E data. *IEEE Trans. Geosci. Remote Sensing, 41*, 243-252

Curry, J.A., W.B. Rossow, D. Randall and J.L. Schramm (1996), Overview of Arctic Cloud and Radiation Characteristics. *J. Climate, 9*, 1731-1764

Deser, C., R. A. Thomas and S. Peng (2007), The transient atmospheric circulation response to North Atlantic SST and sea ice anomalies, *J. Climate, 20*, 4751-4767

Eastman, R., and S.G. Warren, (2010), Interannual variations of Arctic cloud types in relation to

sea ice. *J. Climate, in press*

Evan, A. T.; Liu, Y. and Maddux, B. State of the climate in 2007: Global cloudiness. *Bull. Amer. Meteor. Soc., 89, No. 7*, 2008, S23-S26.

Francis, J.A., W. Chen, D.J. Leathers, J.R. Miller, and D.E Veron, (2009), Winter northern hemisphere weather patterns remember summer Arctic sea ice extent. *Geophys. Res. Lett., 36*, doi: 10.1029/2009GL037274.

Intrieri, J. M., M. D. Shupe, T. Uttal, and B. J. McCarty (2002). An annual cycle of cloud characteristics observed by radar and lidar at SHEBA. *J. Geophys. Res., 107*, doi: 10.1029/2000JC000423

Kato, S., N. Loeb, P. Minnis, J. Francis, T. Charlock, D. Rutan, E. Clothiaux and S. Sun-Mack (2006), Seasonal and interannual variations of top-of-atmosphere irradiance and cloud cover over polar regions derived from the CERES data set. *Geophys. Res. Lett, 33*, doi:10.1029/2006GL026685

Kauker, F., T. Kaminski, M. Karcher, R. Giering, R. Gerdes, and M. Vossbeck, (2009), Adjoint analysis of the 2007 all time Arctic sea-ice minimum. *Geophys. Res. Lett, 36*, 5.

Kay, J. E., and A. Gettelman, (2009), Cloud influence on and response to seasonal Arctic sea ice loss. *J. Geophys. Res*., 114.1

Kay, J. E., L'Ecuyer, T., Gettelman, A., Stephens, G., and C. O'Dell (2008), The contribution of cloud and radiation anomalies to the 2007 Arctic sea ice extent minimum, *Geophys, Res. Lett*., *35*, L08503, doi:10.1029/2008GL033451.

Kwok, R., and D. A. Rothrock (2009), Decline in Arctic sea ice thickness from submarine and ICESat records: 1958–2008, *Geophys. Res. Lett., 36*, L15501, doi:10.1029/2009GL039035.

Liu, Y., J.R. Key, J.A. Francis and X. Wang, (2007), Possible causes of decreasing cloud cover in the Arctic winter, 1982-2000. Geophys. Res. Lett., 34, L14705, doi:10.1029/2007GL030042

Liu, Y., S. A. Ackerman, B. C. Maddux, J.R. Key and R.A. Frey, (2010), Errors in Cloud Detection over the Arctic Using a Satellite Imager and Implications for Observing Feedback Mechanisms. *J. Climate, 23,* 1894-1907.

Mahesh, A., M.A. Gray, S.P. Palm, W.D. Hart and J.D. Spinhirne, (2004), Passive and active detection of clouds: Comparisons between MODIS and GLAS observations. *Geophys. Res. Lett, 31,* L04108, doi:10.1029/2003GL018859.

Perovich, D. K., J. A. Richter-Menge, K. F. Jones, and B. Light, (2008), Sunlight, water, and ice: Extreme Arctic sea ice melt during the summer of 2007. *Geophys. Res. Lett, 35, 4.*

Rigor, I.G., R.L. Colony, and S. Martin, (2000), Variations in surface air temperature observations in the Arctic, 1979–97. *J. Climate, 13,* 896–914.

Santer, B.D., T. M. L. Wigley, J. S. Boyle, D. J. Gaffen, J. J. Hnilo, D. Nychka, D. E. Parker, and K. E. Taylor, (2000), Statistical significance of trends and trend differences in layer-average atmospheric temperature time series, *J. Geophys. Res., 105,* 7337-7356

Schutz, B., H. Zwally, et al. (2005), Overview of the ICESat Mission. *Geophys. Res. Lett., 32,* (L21S01), doi: 10.1029/2005GL024009.

Schweiger, A. J., (2004), Changes in seasonal cloud cover over the Arctic seas from satellite and surface observations. *Geophys. Res. Lett., 31,* L12207, doi:10.1029/2004GL020067.

Schweiger, A.J, R.W. Lindsay, S. Vavrus and J.A. Francis, (2008), Relationships between Arctic sea ice and clouds during autumn, *J. Climate, 21,* 4799-4810.

Serreze, M.C., M.M. Holland and J. Stroeve, (2007), Perspectives on the Arctic's shrinking sea ice cover. *Science, 315,* 1533-1536.

Shupe, M. D. and J. M. Intrieri. (2004), Cloud radiative forcing of the Arctic surface: The influence of cloud properties, surface albedo, and solar angle, *J. Climate., 17,* 616-628.

Skamarock, W.C., Klemp, J.B., Dudhia, J., Gill, D.O., Barker, D.M., Duda, M.G., Huang, X., Wang, W., and Powers, J.G. (2008), A Description of the Advanced Research WRF Version 3. NCAR Technical Note, NCAR/TN-475+STR, June 2008.

Spinhirne, J.D., S.P. Palm, W.D. Hart, D.L. Hlavka, and E.J. Welton, (2005), Cloud and aerosol measurements from GLAS: Overview and initial results. *Geophys. Res. Lett., 32* (22), L22S03, doi:10.1029/2005GL023507.

Strey, S.T., W.L. Chapman, and J.E. Walsh, (2010), The 2007 Sea Ice Minimum: Impacts on the Northern Hemisphere Atmosphere in Late Autumn and Early Winter, *Geophys. Res. Lett*, in press.

Strey, Sara T. (2009), The Effects of an Extreme Arctic Sea Ice Minimum on the Northern Hemisphere Atmosphere During Late Autumn and Early Winter, M.S. thesis, University of Illinois at Urbana-Champaign, Urbana

Stroeve J., M. M. Holland, W. Meier, T. Scambos, and M. Serreze (2007), Arctic sea ice decline: Faster than forecast, *Geophys. Res. Lett., 34*, L09501, doi:10.1029/2007GL029703

Vavrus, S., D. Waliser, A. Schweiger and J. Francis (2009), Simulations of 20th and 21st century Arctic cloud amount in the global climate models assessed in the IPCC AR4. *Clim. Dyn., 33*, 1099-1115.

Wang, X. and J.R. Key, (2003), Recent trends in Arctic surface, cloud and radiation from space. *Science, 299*, 1725-1728.

Wang, X. and J.R. Key, (2005), Arctic Surface, Cloud and Radiation Properties Based on the AVHRR Polar Pathfinder Dataset. Part II: Recent Trends. *J. Climate, 18*, 2575-2593.

Winker, D.M., W.H. Hunt and M.J. McGill, (2007), Initial performance assessment of CALIOP. *Geophys. Res. Lett., 34*, L19803, doi:10.1029/2007GL030135

Figure Captions

Figure 1. ICESat (a) and CALIPSO (b) cloud fraction over water and sea ice for the period October 2 to November 5, 2007 and the AMSR-E measured sea ice fraction (c) for the month of October, 2007. The overall cloud fraction for the region shown is 92.0% for CALIPSO and 93.5% for ICESat. Note that ICESat obtains measurements to 86 N and AMSR-E to the pole, while CALIPSO only to 82 N. The ICESat and AMSR-E data above 82 N are masked out to ensure the cloud and sea ice observations of the three satellites covered the same area.

Figure 2. Average cloud percent for the region shown in Figure 1 from ICESat observation periods (each about 33 days long) beginning in October, 2003 and ending in October of 2007 (pink crosses) and from monthly average CALIPSO measurements (solid black line) from June, 2006 to December, 2008. The dashed black line is CALIPSO cloud percent but only for longitudes between 90 and 270 and north of 70 N. The red line is the average monthly AMSR-E ice coverage (percent) for the same area. Upper thin black line and lower straight red line are trends estimated from the October cloud fraction and sea ice data, respectively.

Figure 3. ICESat measured cloud frequency as a function of height normalized by the total number of cloud observations (a) for clouds that occur over water (solid line) and for clouds that occur over ice (dashed line) and the average 1064 nm cloud optical depth (b) segregated in the same manner. The observations are from October ICESat observation periods of 2003 through 2007

Figure 4. Simulated 2007 atmosphere and ice minus 2007 atmosphere with 1984 ice for the month of October. Upward latent heat flux (a) and planetary boundary layer height (b) are shown.

Figure 5. ICESat and CALIPSO cloud fraction for the October data shown in Figure 2 plotted against the corresponding sea ice amount (sea ice percent over the study area).

Table 1. CALIPSO and ICESat retrieved cloud amount for the Arctic for all 4 overlapping observation periods and 4 sub-regions in the Pacific and Atlantic Ocean for 2 of the 4 overlapping observation periods.

Area	Time Period	CALIPSO Cloud Percent	ICESat Cloud Percent
Arctic	6/8 – 6/23 2006	88.0	89.0
Arctic	10/25 – 11/27 2006	88.4	88.6
Arctic	3/12 – 4/14 2007	76.2	73.8
Arctic	10/2 – 11/5 2007	92.0	93.5
North Atlantic	10/25 – 11/27 2006	68.0	65.5
South Atlantic	10/25 – 11/27 2006	70.7	73.7
North Pacific	10/25 – 11/27 2006	72.5	76.5
South Pacific	10/25 – 11/27 2006	69.5	68.8
North Atlantic	3/12 – 4/14 2007	63.5	67.4
South Atlantic	3/12 – 4/14 2007	70.3	71.6
North Pacific	3/12 – 4/14 2007	69.4	75.1
South Pacific	3/12 – 4/14 2007	69.4	71.9
Mean and Standard Deviation of all Areas and Times:		**74.8, 9.3**	**76.3, 9.1**

Figure 1

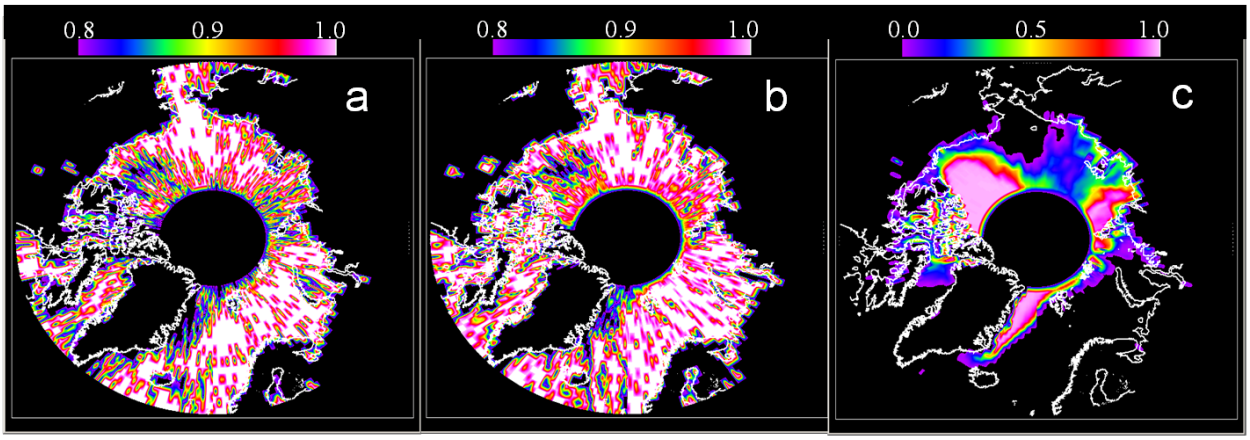

Figure 2

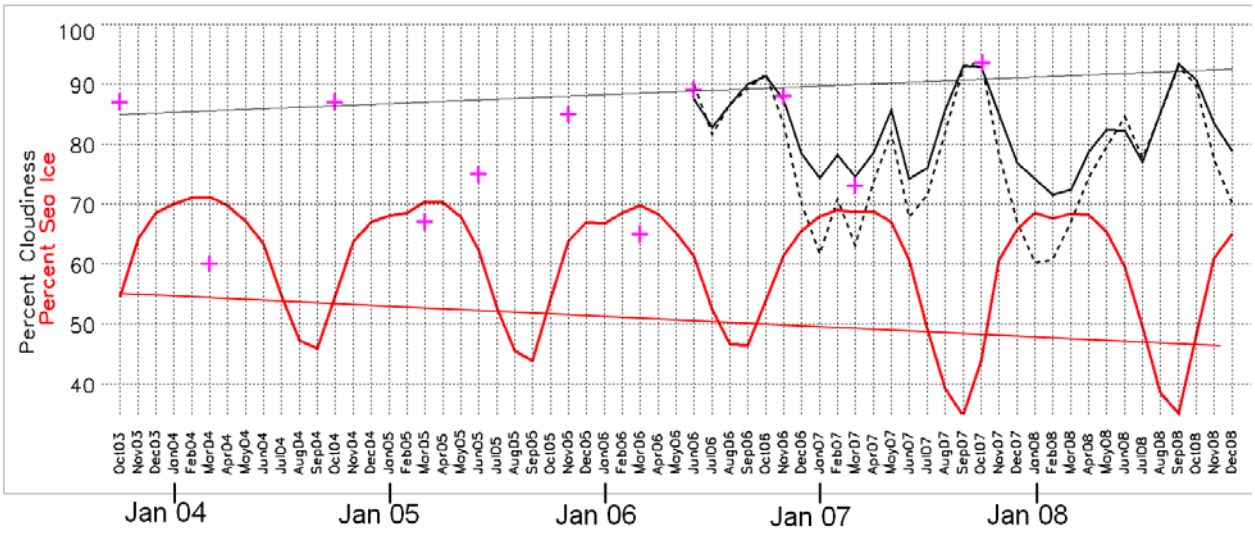

Figure 3

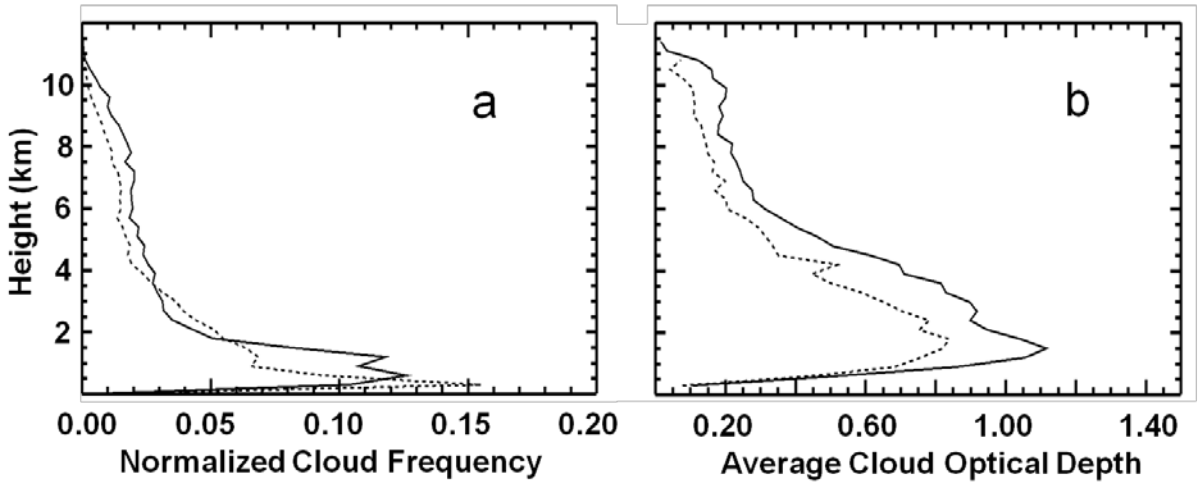

Figure 4.

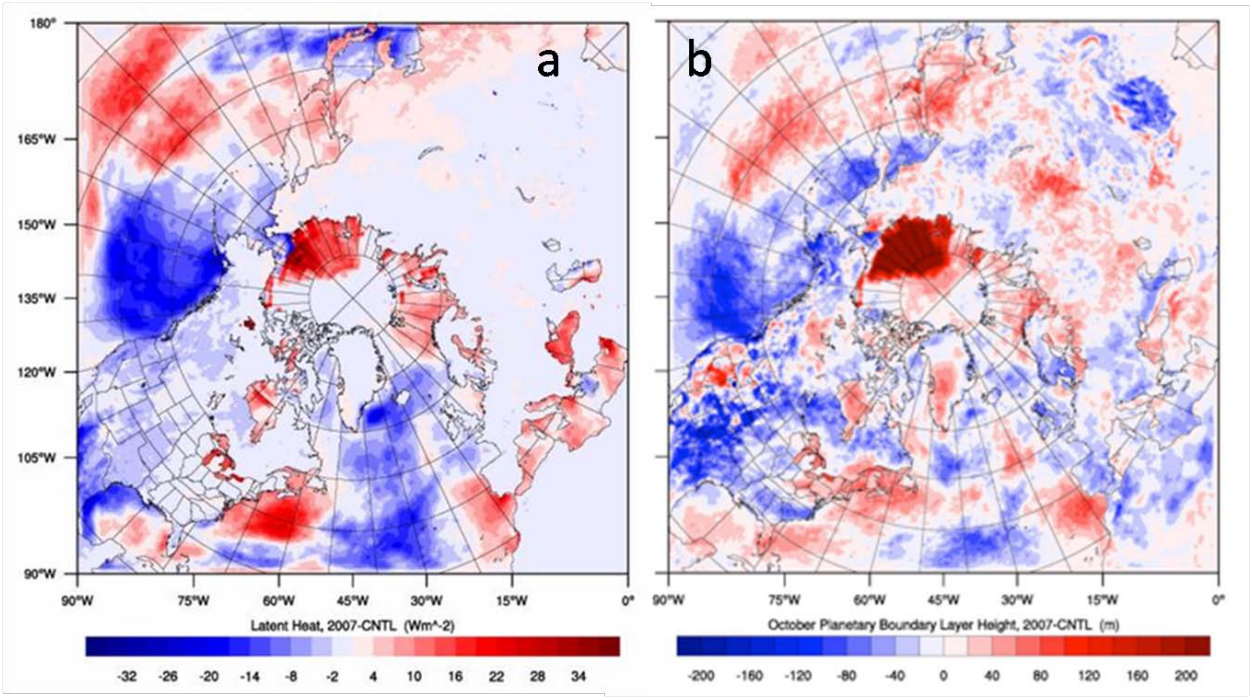

Figure 5

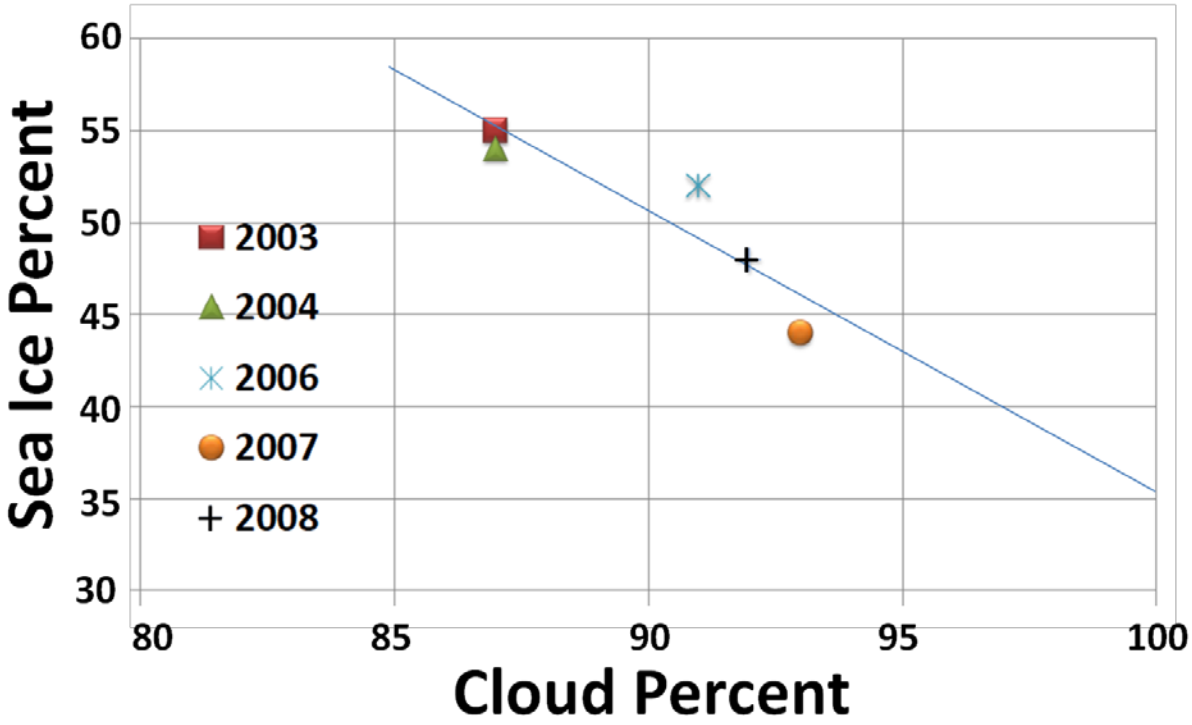
Sea Ice Percent
60
55
50
45
40
35
30
2003
2004
2006
2007
2008
80
85
90
95
100
Cloud Percent